Available online at www.sciencedirect.com

SciVerse ScienceDirect

journal homepage: www.elsevier.com/locate/he

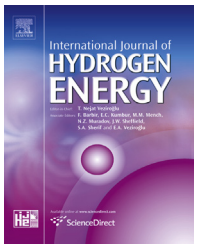

Low cost monitoring system for safe production of hydrogen from bio-ethanol

L. Nieto Degliuomini [a,1], D. Zumoffen [a,b,1], M. Basualdo [a,b,*]

[a] Computer Aided for Process Engineering Group (CAPEG), French-Argentine International Center for Information and Systems Sciences (CIFASIS-CONICET-UNR-AMU), 27 de Febrero 210 bis, S2000EZP Rosario, Argentina
[b] Universidad Tecnológica Nacional – FRRo, Zeballos 1341, S2000BQA Rosario, Argentina

ARTICLE INFO

Article history:
Received 22 February 2013
Received in revised form
29 July 2013
Accepted 14 August 2013
Available online 16 September 2013

Keywords:
Safety hydrogen production
Optimal monitoring system design
Faults in catalyzers
Faults in fuel cell

ABSTRACT

In this paper a monitoring system is developed to guarantee safety operational conditions for the hydrogen production from bioethanol. The key idea is to detect the most critical faults with the minimum number of sensors. It can be done through a fault detectability index (FDI) which drives to the optimal measurements selection for building a proper monitoring system. The FDI calculation is based on principal component analysis (PCA) model with combined statistics. It takes into account those sensors already selected for control purposes and penalizes the use of new measurement devices. The overall methodology is tested for fifteen failures such as the catalyzer deterioration in the reforming reactor, faults at the fuel cell, sensors and actuators. Hence, the investment cost can be reduced drastically without losing quality of fault detection. The monitoring system with the selected sensors by the FDI performs better than using all the available plant measurements.

1. Introduction

The hydrogen production from bio-ethanol involves a highly interconnected plant, named the Fuel Processor System (FPS), to achieve good efficiencies and assure an economically feasible option. For safety considerations the direct reforming of ethanol instead of storing hydrogen is preferred for handling and distributing this fuel [1,2]. Kleme et al. [3] considered that a properly controlled and monitored process derives in better economics indexes and a more ecological operation. However, it is extremely difficult to achieve a suitable monitoring without the support of a decision maker system. In particular, it must be remarked that hydrogen is a dangerous substance because its lower flammability limit has a low value. In Aprea [4] was reported that for hydrogen in air this value is 4% by volume. Mixtures between 4 and 75% are flammable and mixtures between 18.3 and 59% are detonable. In this context, the subject of safety involving production, manipulation and use, is a main concern, as pointed by Aprea [4]. Therefore, any effort focused on added security for handling hydrogen results in a more safe plant, which is always advantageous.

In this context, the detectability indexes are useful for determining a priori which set of variables is enough to

* *Corresponding author*. Computer Aided for Process Engineering Group (CAPEG), French-Argentine International Center for Information and Systems Sciences (CIFASIS-CONICET-UNR-AMU), 27 de Febrero 210 bis, S2000EZP Rosario, Argentine. Tel.: +54 341 4237248 304; fax: +54 341 482 1772.
E-mail address: basualdo@cifasis-conicet.gov.ar (M. Basualdo).
[1] Tel.: +54 341 4237248 304; fax: +54 341 482 1772.

0360-3199/$ – see front matter
http://dx.doi.org/10.1016/j.ijhydene.2013.08.059

achieve the best fault classification. It must be noticed that accounting excessive number of measurements could deteriorate the quality of the fault detection. In Yiang and Xiao [5] and Bhushan et al. [6] the selection of variables to improve the detectability, was addressed. Jeong et al. [7] applied these tools for a Molten Carbonate Fuel Cell of 300 kW. In this work, the detectability index is calculated, based on the PCA model developed opportunely. A PCA-based monitoring system is widely used in industrial processes as well as academic research [8,9]. It is due to their excellent properties for handling noise and large data bases. Finally, through a proper formulation of the genetic algorithm tool is possible to construct an efficient monitoring system. It can be done by formulating an objective function that penalizes the use of new measurement devices that are not in the current control structure. Hence, by this way, it is possible to avoid the use of additional sensors for monitoring purpose because it will increase the hardware investment cost [10].

The methodology used in this work was presented in Zumoffen and Basualdo [11], they applied it to the well known Tennessee Eastman Process. Therefore, a global analysis, generalized and systematic for solving how to design an optimal sensor network integrated to the plant-wide control structure and the optimal monitoring system design was performed. In the previous work of Nieto Degliuomini et al. [12], this methodology was applied on the bio-ethanol processor system. There, an optimal monitoring system design (OMSD), considering typical faults in sensors, was presented. The OMSD was based on historical data base for both, normal and abnormal behavior of the process. In this work, the analysis is extended to more inherent faults such as the catalyzer deterioration in the reforming reactor to produce hydrogen and in the fuel cell (FC). An usual problem in catalyzed reactions is the reduction of the activity, consequently, the conversion of reactions is affected. This diminution could be due to deposition of carbon in the catalyzer, with the consequent reduction of active surface. This is a key fault scenario, and it could be an indicator to consider control reconfiguration, or catalyzer regeneration, which is why it is so important to properly detect. Moreover, three typical faults that can occur with the FC, such as increase in the compressor motor friction, overheating of compressor motor and increase in the fluid resistance are considered too. Hence, these realistic scenarios allow to evaluate the capacity of the OMSD to be extended to another faults too.

The main steps of this methodology are graphically summarized at Fig. 1, showing the involved tools in each stage. In Fig. 1, the block diagram with red background displays the procedure applied in [12], the MSD approach. Meanwhile, the blue background shows the module developed in this work and its integration with the OMSD strategy.

The final checking about the quality of the predictions given by the detectability index is presented. The monitoring system based on PCA with combined statistic [13] is applied here to the dynamic model of the controlled FPS. Therefore, the results presented in this work will be useful to get more insight about the benefits of having an efficient system to determine in time if the most critical faults occur. It constitutes a recommendable way for guaranteeing safety at lower cost and efficiency for the Fuel Processor system with Proton Exchange Membrane Fuel Cell (FPS + PEMFC) which represents one of the new energy paradigms.

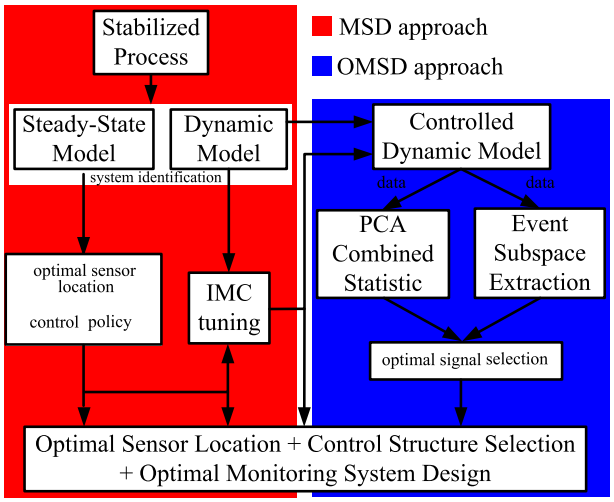

Fig. 1 – Proposed strategy.

2. Fault detectability index

In this section a brief review of the main tools needed for developing an efficient FDI used in this work is detailed.

2.1. *PCA-based monitoring*

The principal component analysis (PCA) is the main tool used here for performing fault detection. PCA is a projection-based method that facilitates a reduction of data dimension. This analysis begins by considering the data matrix $\mathbf{X}$ of $m \times n$ containing m samples of n process variables collected under normal operation. Assuming that $\overline{\mathbf{X}}$ is the normalized version of $\mathbf{X}$, to zero mean and unit variance scaled by parameter vectors $\mathbf{b}$ and $\mathbf{s}$ respectively. The normalized data matrix can be represented as

$$\overline{\mathbf{X}} = \mathbf{T}\mathbf{P}^T + \mathbf{E} \tag{1}$$

where $\mathbf{T} \in \Re^{m \times A}$ and $\mathbf{P} \in \Re^{n \times A}$ are the latent and principal components matrix respectively, and A is the number of principal components retained in the model $\mathbf{P}$. The residual matrix $\mathbf{E}$ represents the associated error since only $A \ll n$ principal components were selected.

$\mathbf{P}$ can be obtained by means of singular value decomposition (SVD) from the normalized data correlation matrix as is shown in (2)

$$\mathbf{R}_c = \overline{\mathbf{X}} \cdot \overline{\mathbf{X}}^T / (m-1) = \mathbf{U}\mathbf{D}_\lambda \mathbf{U}^T \tag{2}$$

by selecting only the first A columns of $\mathbf{U}$. This factorization produces a diagonal matrix $\mathbf{D}_\lambda = \mathrm{diag}(\lambda_1, \lambda_2, \ldots, \lambda_n)$, where λ_i are the eigenvalues of $\mathbf{R}_c$ sorted in decreasing order ($\lambda_1 > \lambda_2 > \ldots > \lambda_n$) and the corresponding columns of $\mathbf{U}$ are the eigenvectors $\mathbf{p}_i$ and so called the principal components. being $\mathbf{P} = [\mathbf{p}_1, \ldots, \mathbf{p}_A]$ and $\mathbf{D}_A = \mathrm{diag}(\lambda_1, \ldots, \lambda_A)$.

A reduction of dimensionality is made by projecting every normalized sample vector $\overline{\mathbf{X}}(k)$ (of dimension $n \times 1$) in the principal component space generated by $\mathbf{P}$,

$$\mathbf{T}(k) = \mathbf{P}^T\overline{\mathbf{X}}(k) \tag{3}$$

which is called the principal score vector.

Different approaches for selecting the A principal components retained [14] can be chosen. In this work the cumulative percent variance (CPV) is used and displayed in (4). This index measures the percent variance captured by the first A principal components.

$$CPV(A) = \frac{\sum_{j=1}^{A}\lambda_j}{\text{trace}(\mathbf{R}_c)}100\% \tag{4}$$

In this case a search between $1 \le A \le n$ is made in order to satisfy the condition $CPV(A) \ge \delta_{cpv}$ with the minimum A. Where δ_{cpv} is a percentage value, if it achieves lower values means that only a few principal components retained are needed and if it is close to 100% means that $A \approx n$.

2.2. Hotelling and square prediction error statistics

For generating quality control charts in multivariable online monitoring process with PCA, two statistics are widely used: the Hotelling, $T^2(k)$, and the squared prediction error (SPE), $Q(k)$ [11,15–17]. Considering the actual process measurements at their normalized version $\overline{\mathbf{X}}(k)$, being k the actual sampling time, these statistics are defined as are shown in (5),

$$T^2(k) = \left\|\mathbf{D}_A^{-1/2}\mathbf{P}^T\overline{\mathbf{X}}(k)\right\|^2, \quad Q(k) = \left\|\tilde{\mathbf{C}}\overline{x}(k)\right\|^2 \tag{5}$$

where $\tilde{\mathbf{C}} = I - \mathbf{P}\mathbf{P}^T$ and $\Delta\overline{\mathbf{X}}(k) = \tilde{\mathbf{C}}\overline{x}(k)$ is the prediction error.

The test consists on declaring as normal operation if $T^2(k) \le \delta_{T^2}$ for Hotelling's statistic and $Q(k) \le \delta_Q$ for SPE statistic. Where δ_{T^2} and δ_Q are the control or confidence limits for the above statistics respectively. Supposing a Gaussian distribution the control limits can be approximated by $\delta_i = \mu_i + \nu\cdot\sigma_i$ [18,19], where μ_i and σ_i are the mean and variance values for the statistic i computed from the normal data matrix ($i = T^2$,Q) and $\nu = 2,3$ according to the 95% or 99% confidence level respectively.

The model, $\mathbf{P}$, is computed using the normal data matrix, which has information about the *common-cause* variations at the surroundings of the process operation point. The Hotelling's statistic, T^2, for a new incoming data sample is a measurement of its distance respect to the origin of the dominant variation subspace. This origin and its proximities delimit the *in-control zone*. In case that an abnormal event happens but the principal score vectors remain at the surroundings of the in-control zone (Hotelling's statistic is under the confidence limit) suggests that it can not change enough over the dominant variation subspace to advice about the occurrence of that abnormal event. The use of the Q and T^2 statistics, working together, in a combined way [13] could be able to avoid this lose of detection. Hence, in Section 2.4 a new detectability analysis is done based on the combined statistics. This approach improves the detection properties such as detection times, less false alarms occurrence and missed detections.

2.3. Fault detectability index based on T^2 and Q

Fault detectability index can be suitably obtained by using an additive fault model representation of the abnormal process data. This methodology can be applied to both Hotelling (T^2) and the square prediction error statistics (Q). Yue and Qin [13] presented an approach to develop this index but for T^2 and Q separately. In the next sections an extension of it for computing the fault detectability index based on the combined statistics is proposed.

The normalized process measurement, $\overline{\mathbf{X}}_*(k)$, when a fault is present can be written as,

$$\overline{\mathbf{X}}_*(k) = \overline{\mathbf{X}}_0(k) + \Theta_j\mathbf{f}_j \tag{6}$$

in this fault model can be observed two additive effects: $\overline{\mathbf{X}}_0(k)$ that considers the normal behavior case and $\Theta_j\mathbf{f}_j$ as the fault contribution to the actual measurements. Being Θ_j the fault subspace for the fault j with $j = 1,\ldots,J$ the fault types and $\mathbf{f}_j$ the fault components vector.

$$\begin{bmatrix}\overline{x}_*^1(k)\\ \overline{x}_*^2(k)\\ \vdots\\ \overline{x}_*^n(k)\end{bmatrix} = \begin{bmatrix}\overline{x}_0^1(k)\\ \overline{x}_0^2(k)\\ \vdots\\ \overline{x}_0^n(k)\end{bmatrix} + \begin{bmatrix}\theta_j^{11} & \theta_j^{12} & \ldots & \theta_j^{1r}\\ \theta_j^{21} & \theta_j^{22} & \ldots & \theta_j^{2r}\\ \vdots & \vdots & \vdots & \vdots\\ \theta_j^{n1} & \theta_j^{n2} & \ldots & \theta_j^{nr}\end{bmatrix}\begin{bmatrix}f_j^1(k)\\ f_j^2(k)\\ \vdots\\ f_j^r(k)\end{bmatrix} \tag{7}$$

where n is the amount of measurement points, and r the fault components vector length for the fault type j. The columns of Θ have zero entries except for the measurement affected by the fault, in this case the entry is 1 or -1 depending of the fault direction.

The fault detectability condition with Q statistic is summarized as

$$\left\|\tilde{\mathbf{C}}\Theta_j\mathbf{f}_j\right\| \ge 2\delta_Q \tag{8}$$

where $\mathbf{C}$ is the prediction error matrix, and δ_Q the control limit. Then, in this case, the detectable Minimal Fault Magnitude (MFM) estimation results

$$\left\|\mathbf{f}_j\right\|_{MFM}^{Q} = \left\|\tilde{\mathbf{C}}\Theta_j\right\|^{-1}2\delta_Q \tag{9}$$

Equations (8) and (9) summarizes the detectability and MFM only for the SPE. An analogous analysis can be made for the Hotelling statistic.

2.4. Fault detectability index based on combined statistic

The combined index $z(k)$ is defined as shown at (10),

$$z(k) = \frac{T^2(k)}{\delta_{T^2}} + \frac{Q(k)}{\delta_{SPE}} \tag{10}$$

note that $z(k)$, $T^2(k)$ and $Q(k)$ are the computed statistics for the actual measurement $\overline{\mathbf{X}}(k)$. Under these assumptions can be declared as normal operation condition if $z(k) \le \delta_z$, where δ_z is the new control limit. A conservative selection could be $\delta_z = 2$, according to the false alarms occurring when the fault detection system is injurious.

In this subsection, the development of the fault detectability index with the combined statistic, $z(k)$, is given. It is done by performing an extension of the concepts given in the previous section. By grouping both Hotelling and square

prediction error statistics can be obtained improvements in the fault detection performance [11,15–17]. In this case, the combined statistic can be represented as

$$z(k) = \frac{\overline{\mathbf{X}}_*^T(k)\mathbf{P}\mathbf{D}_A^{-1}\mathbf{P}^T\overline{\mathbf{X}}_*(k)}{\delta_{T^2}} + \frac{\overline{\mathbf{X}}_*^T(k)\tilde{\mathbf{C}}^T\tilde{\mathbf{C}}\overline{\mathbf{X}}_*(k)}{\delta_Q}$$
$$= \overline{\mathbf{X}}_*^T(k)\left[\frac{\mathbf{P}\mathbf{D}_A^{-1}\mathbf{P}^T}{\delta_{T^2}} + \frac{\tilde{\mathbf{C}}^T\tilde{\mathbf{C}}}{\delta_Q}\right]\overline{\mathbf{X}}_*(k) = \overline{\mathbf{X}}_*^T(k)M\overline{\mathbf{X}}_*(k) \quad (11)$$

with

$$M = \left[\frac{\mathbf{P}\mathbf{D}_A^{-1}\mathbf{P}^T}{\delta_{T^2}} + \frac{\tilde{\mathbf{C}}^T\tilde{\mathbf{C}}}{\delta_Q}\right] \quad (12)$$

considering that $\mathbf{M}$ is a symmetric and definite positive matrix [13], is possible its decomposition by Cholesky factorization to obtain $\mathbf{M} = \mathbf{R}^T\mathbf{R}$. Thus, the combined statistic case presents a similar treatment as the Q statistic in Section 2.3, giving the following fault detectability condition

$$\left\|\mathbf{R}\Theta_j\mathbf{f}_j\right\| \geq 2\delta_z \quad (13)$$

and its corresponding MFM estimate

$$\left\|\mathbf{f}_j\right\|_{MFM}^z = \left\|\mathbf{R}\Theta_j\right\|^{-1}2\delta_z \quad (14)$$

The combined matrix $\mathbf{M}$ (and eventually $\mathbf{R}$) depends on the PCA model developed opportunely. The influences of factors such as sensors location in the process, signals selection to perform PCA model, variance retained, and confidence limits are crucial and limit the attainable MFM. Similarly, the fault subspace matrix Θ_j is directly influenced by the sensors network (potential sources of faults) and the selected control structure. In other words, a particular design of these matrices can incur on losses or poor quality fault detections. In Zumoffen and Basualdo [11] is presented an application to large scale plants where a comparison is suggested between a PCA model developed using the overall available measurements with other based on maximizing fault detectability with and optimal number of signals.

3. Optimal monitoring system design (OMSD)

The methodology proposed by Zumoffen and Basualdo [11] is graphically shown at Fig. 1. The approach stated in Nieto Degliuomini et al. [12] (MSD) allows to find a proper plant-wide control structure being the first step selecting the variables to be measured. Basically, the MSD approach defines,

- the hardware requirements: amount and type of sensors and controllers which are potential sources of faults,
- the control structure: how disturbances and abnormal events affect (are masked by the control) the overall process behavior,

Then, from MSD all the available measurements for control purpose are candidates to be selected to be used by the OMSD.

3.1. Optimal signal selection based on detectability maximization

The proper signals selection for the PCA model development is performed by focusing on faults detectability maximization. It is based on the existing sensors network in the previously proposed optimal control structure in [12] (MSD) and the potential additional cost in case that new measurement points would be required.

In this context, the problem can be defined as follows, considering N_c available signals including controlled as well as manipulated variables in the process and $\mathbf{C}_i = [c_1, c_2, \ldots, c_{Nc}]$ a particular signals selection, where $c_l = \{1; 0\}$ with $l = 1,\ldots,N_c$ represents a binary alphabet indicating the utilization or not of the signal in the l location. Then, the PCA model construction depends on this particular selection, $\mathbf{P}(\mathbf{C}_i)$ and $\mathbf{D}_A(\mathbf{C}_i)$. In addition, the MFM calculation when combined statistics are used results

$$\|\mathbf{f}_j^i\|_{MFM}^z = \left\|\mathbf{R}(\mathbf{C}_i)\Theta_j(\mathbf{C}_i)\right\|^{-1}2\delta_z \quad (15)$$

where i makes reference to the signals selection $\mathbf{C}_i$, with $i = 1,\ldots,2^{N_c}$ all the possible combinations and $j = 1,\ldots,J$ the considered abnormal events types (disturbances, faulty elements, etc.).

A cost penalization $\mathbf{c} = [c_1^*, \ldots, c_{N_c}^*]$, greater than zero each time that extra measurements, not already included for the control structure, are recommended to be selected. Note that $\mathbf{c}$ can be selected tacking into account a tradeoff between detectability and quantity of new sensors. Thus, lower values of $\mathbf{c}$ means that the minimization of the objective function in (16) priories detectability without considers the cost of extra sensors. Otherwise, when $\mathbf{c}$ has a considerable weight the cost of new sensors is penalized without considers the detectability index. The penalization coefficients must be normalized to contribute in the same order of magnitude of the term $\left\|\mathbf{R}(\mathbf{C}_i)\Theta_j(\mathbf{C}_i)\right\|^{-1}2\delta_z$. Therefore, the complete problem to be solved can be stated as

$$\min_{\mathbf{C}_i}\left[\sum_{j=1}^{J}\|\mathbf{f}_j^i\|_{MFM}^z + \mathbf{c}\mathbf{C}_i^T\right] = \min_{\mathbf{C}_i}\left[\sum_{j=1}^{J}\left\|\mathbf{R}(\mathbf{C}_i)\Theta_j(\mathbf{C}_i)\right\|^{-1}2\delta_z + \mathbf{c}\mathbf{C}_i^T\right] \quad (16)$$

According to the combinatorial characteristic (16) has 2^{N_c} potential solutions. In addition, the minimization of the MFM with combined statistics in (16), drives to the maximization of the faults detectability. In other words, the search is oriented towards to find the optimal signals selection $\mathbf{C}_{op}$ (solution of (16)) that guarantees the best fault detection of the most expected abnormal events at a lowest investment cost.

Then, the data base from the controlled plant (or eventually from the dynamic model) is processed and analyzed. The data corresponding to a normal behavior is used to develop the PCA model with combined statistic. On the other hand, the abnormal data base is analyzed to build the event/fault subspace, Θ, can be extracted by processing the overall potential measurements and signals from the process. Initially, due to the typical noise present in the process measurements is applied a smoothed moving average (SMA) filter for consistence. It performs the average (mean) of the original signal $x(k)$

over a specified moving window of dimension $N+1$ samples, as can be observed in (17), resulting in the filtered version $x_f(k)$.

$$x_f(k) = (N+1)^{-1} \sum_{i=0}^{N} x(k-i) \tag{17}$$

an improved algorithm exists to avoid problems with lagged samples called exponential weighted moving average (EWMA) for on-line applications [20,18]. Thus, the data base is pre-processed by auto-scaling and then filtering using eq. (17). After this procedure, the fault subspace extraction is performed to obtain the faults direction.

The faults direction are computed using the well-known "*3δ edit rule*" [21] which suggests that if $|x_f(k)| > 3$ the variable is considered to be deviated from its normal state. Analyzing the overall data base for each abnormal case, the fault directions can be computed as

$$F(j,i) = \begin{cases} 1, & \text{if} \quad \bar{x}_f^{ji}(k_*) > 3; \\ 0, & \text{if} \quad -3 \le \bar{x}_f^{ji}(k_*) \le 3; \\ -1, & \text{if} \quad \bar{x}_f^{ji}(k_*) < -3. \end{cases} \quad \text{with} \quad \begin{matrix} j = 1,\ldots,J \\ i = 1,\ldots,N_c \end{matrix} \tag{18}$$

where $\bar{x}_f^{ji}(k_*)$ is the auto-scaled and filtered version of the variable number i from the abnormal data base (event) j evaluated in the sampled instant k^*. This temporal instant is specified according to the dynamic response of the process trying to avoid the transient behavior due to the fault occurrence $k^* = t_f + N^*$. Where t_f is the fault occurrence sample. Thus each row of F represented by $F(j,1{:}N_c)$ corresponds to the j fault propagation over the N_c variables analyzed from the abnormal data base. The faults subspace Θ can be computed directly from the fault direction matrix F as can be observed in (19)

$$\Theta_j = \mathrm{nzr}\{\mathrm{diag}[F(j,1:N_c)]\}^T \tag{19}$$

where the function diag(•) takes the vector $F(j,1{:}N_c)$ as input argument and gives back a diagonal matrix of $N_c \times N_c$ with $F(j,1{:}N_c)$ in its diagonal. On the other side, the function nzr{•} takes as input argument the diagonal matrix constructed previously and gives back another matrix Θ_j. This fault subspace matrix contains only the *non zero rows* from the original diagonal matrix. Finally, this fault propagation matrix can be applied as has been stated in section 2.3.

An alternative approach to obtain the fault direction matrix F exists [11,15–17]. In these works, a strategy based on fuzzy logic tools is applied and the resultant matrix rules represents the fault propagations over the process variables. In this case, the matrix rules evaluation accounts the mean contribution of the variables within the specified zone of analysis.

3.2. *Genetic algorithm solution*

Genetics Algorithms are used here for solving the problem displayed in (16) subject to the following restrictions

$$\begin{aligned} &\sum_{l=1}^{N_c} \mathbf{C}_i(l) > A \\ &\left\| \mathbf{R}(\mathbf{C}_i)\Theta_j(\mathbf{C}_i) \right\| > 0 \end{aligned} \tag{20}$$

where the first restriction in (20) avoids the selection $\mathbf{C}_i$ that does not present dimensional reduction. In addition, if the signal dimension is equal to the principal components retained A the combined statistic z is reduced to Hotelling statistic only (Q = 0). The second constraint avoids the individual selection $\mathbf{C}_i$ that produces $\left\| \mathbf{f}_j \right\|_{MEM}^{z} = \infty$, which means that a specific fault can not be detected. In other words, the second constraint guarantees the fault detectability condition in (13).

This kind of optimization is generally known as combinatorial problem and may have serious drawbacks with the dimension overgrowth which is very common in industrial processes. Different approaches exist to solve this kind of problems: integer optimization, mixed-integer optimization and stochastic search, among others. In this work genetic algorithms for stochastic global search is preferred, because of the reasons mentioned earlier. Also, GA are able to give a set of solutions sorted by the benefit provided by each one in terms of the minimization of the chosen cost function. Hence, the first one is the optimal solution, and the following correspond to the less profitable possibilities. Then, the OMSD approach is completed by including the detectability index for combined statistic, investment cost and Genetic Algorithms to define the optimal signals selection.

4. Application results for hydrogen production with fuel cell

The fuel processor system (FPS) can be seen in Fig. 2. It consists of a Bio-Ethanol Steam Reforming (ESR) plug flow reactor, where most of the conversion of ethanol to H_2 is made. Carbon monoxide which poisons the fuel cell catalyst is produced in the ESR, so additional processing is needed to remove this substance. There are three reactors that configure the cleaning system; these are two Water Gas Shift (WGS), one of high temperature (fast) and the other of low temperature, that favors the equilibrium of the reaction to higher conversion rates of CO. The third is a Preferential Oxidation of Carbon monoxide ($COPrO_x$) reactor, where oxidation of CO into CO_2 is made; also, the undesired oxidation of hydrogen occurs, so the catalyst is selected to improve the conversion of CO. This plant was deeply studied in [22], so, further details about the dynamic modeling, control structure, process constraints and normal behavior can be seen there.

In Table 1 are summarized the available variables in the FPS + FC plant, with 16 potential measurements, 7 of them (y_1,y_3,y_7,y_9,y_{10},y_{11},y_{15}) correspond to the control structure shown at Fig. 2, so they have the sensors installed. A first version of the optimal monitoring system design was based on maximizing the abnormal event detectability by tacking into account the optimal signal selection for constructing a representative PCA model. Seven potential sensor faults, $F_1$to F_7, presented at Table 2 were considered in [22]. They consisted of abrupt bias/offset (step type) within specific range of magnitude. All these sensors (y_1,y_3,y_7,y_9,y_{10},y_{11},y_{15}) were assumed with a normal noise distribution and magnitude between [0.5,5]%respect to their operating points. The following four possible process faults, are: F_8, a catalyst poisoning, and $F_9$to $F_{11}$are related to the Fuel Cell and its compressor. The last four faults taken into account, F_{12} to F_{15}, are manipulated variables (valves) with sticking problem. This

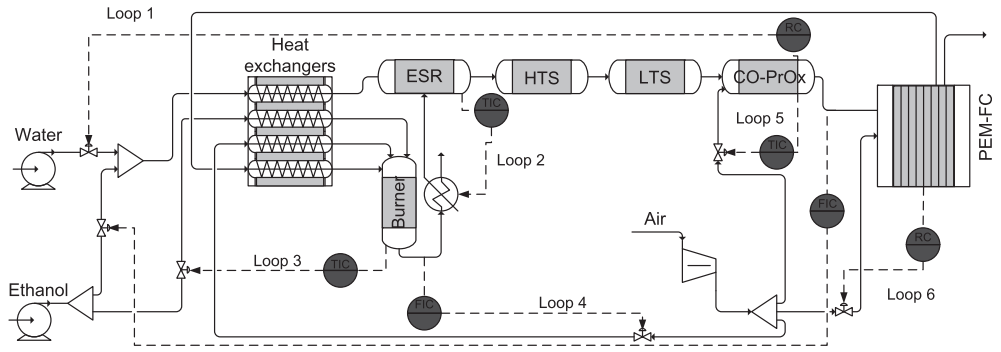

Fig. 2 – Bio-ethanol processor system with controllers.

work is mainly dedicated to extend the previous system given in [22], analyze faults $F_8$to $F_{15}$and check if the same measurements selection is able to present similar detectability properties. Then, the previous results for $F_1$to $F_7$are summarized at Table 5.

According to the data given at Table 1 (measurements and manipulated variables) the combinatorial problem has dimension $N_c = 23$ and $2^{23} \approx 8.3 \times 10^6$ possible solutions. Clearly an exhaustive evaluation of the problem is unpractical. In this context, GA is used to solve the combinatorial problem stated in (16) with the constraints given in (20). The first step for solving this problem is the fault subspace, Θ, extraction by using the methodology stated previously. In this case a modification is introduced to the 3δ-edit rule of (18) for robustness issues. In fact, the fault directions are computed accounting the mean value of the filtered version data in a zone analysis, $[k_i,k_f]$, instead of a single time instant, k^*. Thus, the approach in (18) becomes,

$$F(j,i) = \begin{cases} 1, & \text{if} \quad \text{mean}\left[\bar{x}_f^{ji}([k_i,k_f])\right] > 2 \\ 0, & \text{if} \quad -2 \le \text{mean}\left[\bar{x}_f^{ji}([k_i,k_f])\right] \le 2 \\ -1, & \text{if} \quad \text{mean}\left[\bar{x}_f^{ji}([k_i,k_f])\right] < -2 \end{cases} \tag{21}$$

Table 1 – Variables in the FPS + FC process.

Potential measured		Manipulated	
y_1	ESR exit temperature	u_1	Water to ESR inlet
y_2	Jacket exit gases temperature	u_2	Exchanged heat Q
y_3	Burner exit temperature	u_3	Ethanol to Burner
y_4	Burner entering molar flow	u_4	Oxygen to Burner
y_5	Molar ratio H_2O/Ethanol	u_5	Ethanol to ESR
y_6	HTS exit temperature	u_6	Oxygen to CO-PrO$_x$
y_7	H production rate	u_7	CM voltage
y_8	LTS exit temperature		
y_9	CO-PrO$_x$ exit temperature		
y_{10}	Molar ratio O_2/CO		
y_{11}	Burner exit molar flow		
y_{12}	ESR exit molar flow		
y_{13}	CO-PrO$_x$ CO exit concentration		
y_{14}	Net power		
y_{15}	Oxygen excess		
y_{16}	Stack voltage		

similarly to the fuzzy approach presented in [15–17] the zone analysis allows to obtain a mean contribution of the process variables and to know the trends and effects of abnormal events in a closed loop context. Obviously, this zone is determined according to the plant dynamic responses and taking into account the slower responses.

With the fault subspace, Θ, already obtained, the next step is to solve the optimization problem stated in (16) and (20). In this case, the GA approach is selected and the used parameters setting are shown in Table 3. In Refs. [11,23] a complete analysis of how the initial population, N_i, generation number, N_g, mutation probability, P_m, crossover probability, P_{co}, and the weighting parameters, c_i^* affect the solution of the problem was done. For example, the unweighted, $c_i^* = 0$, and the slightly weighted, $c_i^* = 0.5$, cases propose the same solutions to the problem. The optimal signal selection to maximize detectability is $[y_1,y_3,y_{14},u_1,u_2,u_3,u_6,u_7]$. Taking into account Table 1, this optimal solution suggests the use of a new sensor for the variable y_{14} (net power in the FC). On the other hand, the strongly weighted, $c_i^* = 5$, is focussed on penalizing the new hardware utilization more aggressively. In this context, the optimal solution is $[y_1,y_3,y_{15},u_1,u_2,u_3,u_6,u_7]$, with the benefit that it does not require new measuring points. Thus, this solution only uses the already installed hardware to perform and improve the PCA based monitoring.

In the following, a comparison of three different signals selection for PCA based monitoring shown at Table 4 is performed. The first solution, represented here with the chromosome $\mathbf{C}_{op}$, is the optimal one obtained from the combinatorial problem in (16) and (20), by using the parameters setting displayed in Table 3. There are different solutions that can maximize the fault detection with the use of a small number of sensors, as pointed out in section 3.2. The solution given by the genetic algorithm is not unique, it gives a number of chromosome combinations (solutions) ranked by performance, and we choose the first one ($\mathbf{C}_{op}$) to evaluate, but the others should be providing similar results. The second signals selection to be compared is the so called, $\mathbf{C}_{unf}$, it represents an unfeasible solution and does not fulfill with the detectability condition (second constraint in (20)). Finally, the third solution is named, $\mathbf{C}_{full}$, it considers all possible measurement points and available signals to build the PCA model.

That full solution clearly presents an increase in the cost due to the new measurement points and this sensor network

Table 2 – Abnormal events proposed.

Faults	Variable	Range [%]
F_1	Molar ratio O/CO	±5
F_2	ESR exit temperature	±1
F_3	Burner exit temperature	±3
F_4	Burner exit molar flow	±5
F_5	H_2 production rate	±5
F_6	CO-PrOx exit temperature	±1
F_7	Oxygen excess	±5
F_8	Catalyst surface	±40
F_9	Compressor motor friction	±5
F_{10}	Compressor motor temperature	±20
F_{11}	Fluid resistance	±20
F_{12}	Water to ESR	±5
F_{13}	Oxygen to burner	±5
F_{14}	Bio-ethanol to ESR	±5
F_{15}	Compressor motor voltage	±5

does not guarantee an optimal performance from the monitoring point of view. It seems to indicate that the amount of measurements is not directly related to the quality of fault detection. The last approach is the classical method, but generally not the optimal solution. In fact, we will see here that optimal signals selection with the lowest hardware requirements can match and even improve the performance of the full solution from a PCA based monitoring system point of view. For this comparison the PCA model construction has been made accounting the following common parameters for the three signals selection: cumulative percentage variance, $\delta_{cpv} = 90\%$; confidence limits for T^2 and Q, 99%; z control limit, $\delta_z = 2$. This setting produces that the following principal components retained are (for each solutions): $A_{op} = 5$, $A_{unf} = 7$ and $A_{full} = 10$.

The results obtained for the first seven faults with the parameters given above are summarized in Table 5, with some of the main indicators. For each fault and monitoring system, it is presented the time detection, which is the time that the system takes to detect the faults; the reliability index (RI), which considers the amount of samples that are over the confidence/control limit in percentage mode; the ability to detect the fault; and the most affected variable. For all seven faults, the optimal monitoring system designed, is able to detect them. For faults F_1, F_3 and F_6 the unfeasible system is useless, and of particular interest is fault F_3 where the optimal system is the only one capable of detection, demonstrating that the classical approach of using all variables sometimes deteriorates the quality of monitoring, and can be improved with less capital investment in sensors. Generally, the optimal design is slower in determining the fault occurrence. In the following, new faults are considered, regarding inner process faults, and problems in the manipulated variables, expanding the results obtained previously in [22].

Table 3 – GA Parameters Setting.

N_i	N_c	J	N_g	P_m	P_{co}	Selection	Crossover	c_i^*
3000	23	7	40	$0.7/N_c$	0.7	Roulette wheel	Double-point	5

Table 4 – Different signals selection.

Chromosome	Signals selection
$\mathbf{C}_{op}$	$[y_1,y_3,y_{15},u_1,u_2,u_3,u_6,u_7]$
$\mathbf{C}_{unf}$	$[y_1,y_3,y_4,y_6,y_9,y_{12},y_{13},y_{14},u_2,u_4,u_7]$
$\mathbf{C}_{full}$	$[y_1,y_2,\ldots,y_{16},u_1,u_2,\ldots,u_7]$

The eighth faulty scenario is shown in Fig. 3. This fault represents a catalyst surface diminution in the ESR of 40%, which can be produced by carbon deposition, with the consequent deactivation, due to the minor surface exposed for reaction. In Fig. 3(a) the temporal evolution of the combined statistic z(t) is shown for the full, optimal and unfeasible configurations. In this particular case, $\mathbf{C}_{unf}$ is unable to detect the abnormal event, while the others are able to recognize it rapidly. Moreover, $\mathbf{C}_{full}$ detects the fault with no delay and practically no probability of miss detection, while $\mathbf{C}_{op}$ needs a little more time to detect the event. The variable that presents the major contribution to the fault is y_6, which is shown in Fig. 3(b), it corresponds to the exit temperature of the HTS.

Another fault simulation is shown in Fig. 4. It corresponds to an increase in the compression motor friction, which is represented by an increment in the compressor constant k_v of 5%, producing a reduction in the compressor torque τ_{cm}. Fig. 4 shows the evolution of the combined statistic for the three configurations analyzed. In this case all of them are able to detect a problem in the system, however, the most notorious change is in the optimal configuration because it is not affected by superfluous measurements. The major contribution to the detection is given by u_7, the compressor motor voltage. This fault only affects the FC, so the variable that controls the amount of air injected in the cathode is in charge of rejecting this abnormality.

Table 5 – Indicators for the first seven faults.

Fault	Design	T_d	RI[%]		Variable
F_1	Full	0.65	96.8	✓	u_1
	Unf	–	1.0	x	
	Opt	1.0	72.4	✓	
F_2	Full	0.0	100.0	✓	y_6
	Unf	0.0	100.0	✓	
	Opt	0.0	99.4	✓	
F_3	Full	–	8.6	x	u_3
	Unf	–	0.2	x	
	Opt	0.6	94.4	✓	
F_4	Full	0.3	99.0	✓	u_4
	Unf	0.3	96.8	✓	
	Opt	0.8	96.8	✓	
F_5	Full	0.1	99.6	✓	u_1
	Unf	0.25	89.2	✓	
	Opt	0.45	97.8	✓	
F_6	Full	0.6	85.6	✓	u_6
	Unf	–	1.8	x	
	Opt	1.3	43.6	✓	
F_7	Full	0.05	99.0	✓	y_{16}
	Unf	0.3	99.0	✓	
	Opt	0.3	99.8	✓	

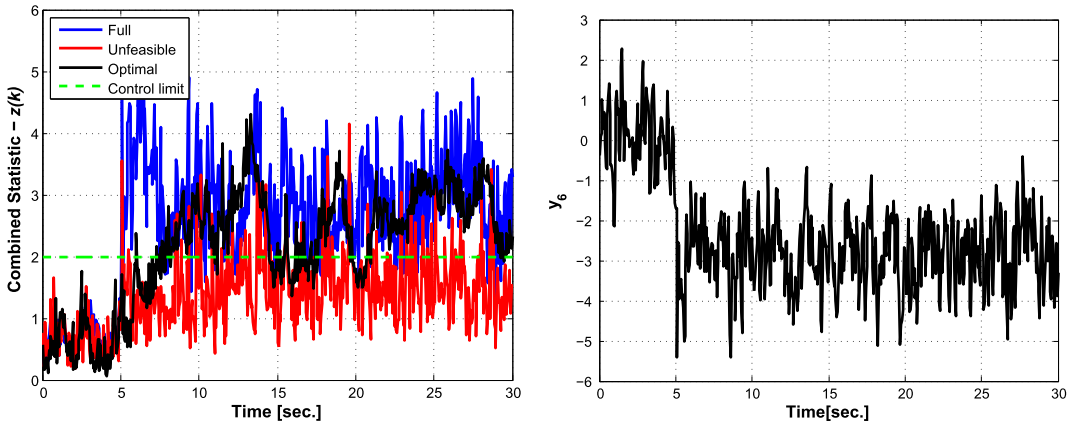

(a) Combined statistic (b) Normalized HTS temperature - y_6

Fig. 3 – Fault F_8 (Catalyst surface diminution −40%).

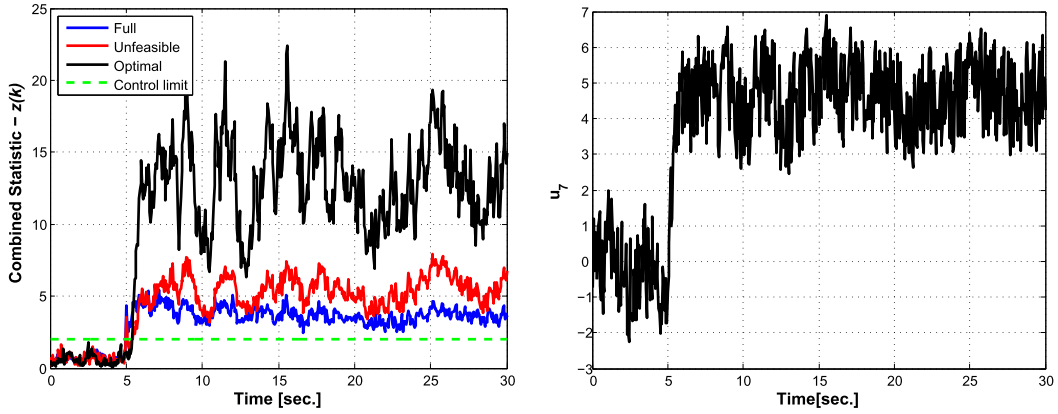

(a) Combined statistic (b) Normalized compressor motor voltage - u_7

Fig. 4 – Fault F_9 (increase of the compressor motor friction +5%).

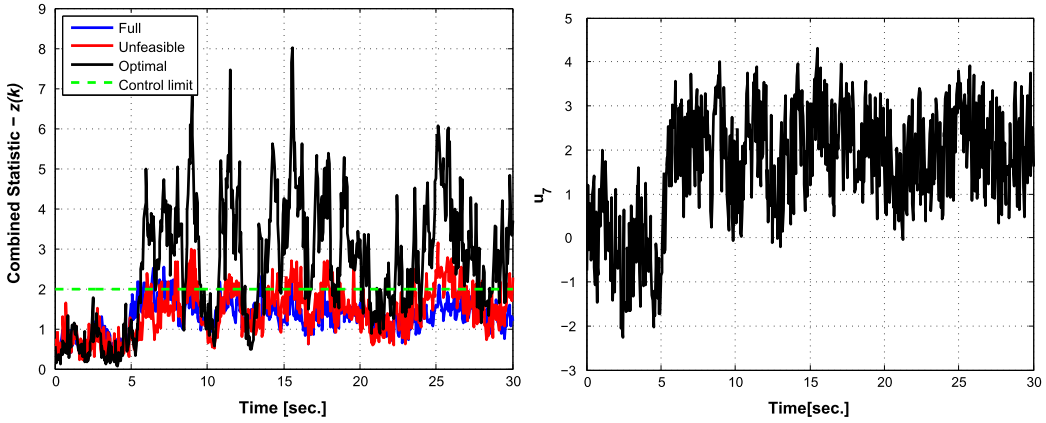

(a) Combined statistic (b) Normalized compressor motor voltage - u_7

Fig. 5 – Fault F_{10} (overheating of the compressor motor +20%).

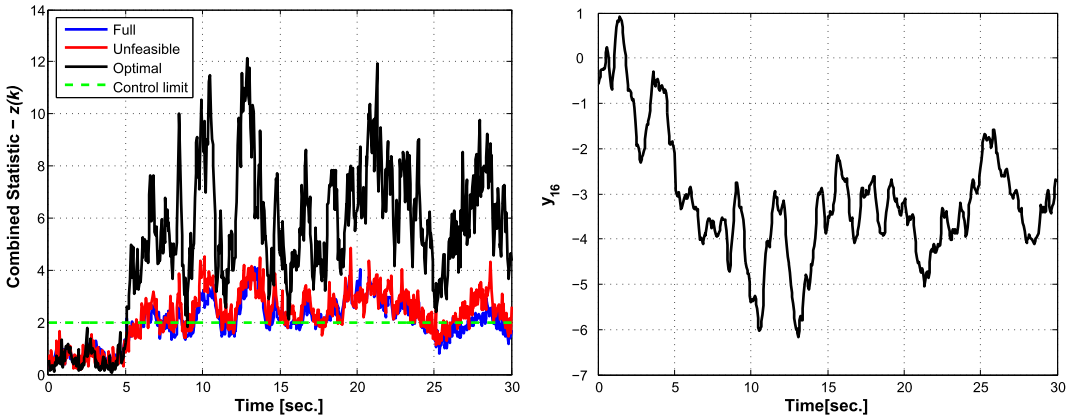

(a) Combined statistic (b) Normalized stack voltage - y_{16}

Fig. 6 – Fault F_{11} (the fluid resistance increases +20%).

Fig. 5 corresponds to the tenth fault analyzed, it consists of an overheating of the compressor motor. It is simulated with an increment in the compressor motor resistance R_cm of 20%, producing a diminution in the compressor torque τ_{cm}. In Fig. 5(a) the value of the combined statistic $z(t)$ is shown. It can be seen that for the optimal variables selection, the fault detection is achieved, but for the unfeasible and the full case is not possible, resulting in a clear miss detection. These results demonstrate again that the full case is a bad solution from the detectability point of view, outperformed by the optimal selection of variables to monitor. Like fault number 9, this abnormal event is local to the FC, and the most affected variable is u_7, shown in Fig. 5(b). The FC is forced to a new operating point in order to reject this disturbance.

The eleventh fault simulated is shown in Fig. 6, corresponds to an increase in the fluid resistance. It is represented with an increase in the orifice constant of the cathode output, $k_{ca,out}$, which produces a proportional change in the outlet air flow in the cathode, $W_{ca,out}$. The evolution of the combined statistic is shown in Fig. 6(a) for the analyzed cases. With the optimal variables selection the fault detection is fast and clear, taking a value over the control limit along the abnormal behavior presence. The cases of full and unfeasible selection are unable to clearly detect the operation out of normal conditions, they oscillate around the control limit, presenting a doubtful performance. For this case, the full solution (usual approach) is as poor as the unfeasible solution considered. The variable that is mainly affected in this scenario is y_{16}, shown in Fig. 6(b), corresponding to the normalized stack voltage.

These last three faults were also analyzed for the same fuel cell but disconnected from the plant, applying model-based diagnosis technique in [22]. The principle of model-based fault detection is to check the consistency of the observed behavior while fault isolation tries to isolate the component that is in fault. The consistency check is based on computing residuals obtained from measured input signals and outputs and the analytical relationships obtained by system modeling. It is remarkable that applying the residuals methodology it was necessary the use of four signals for detecting the three

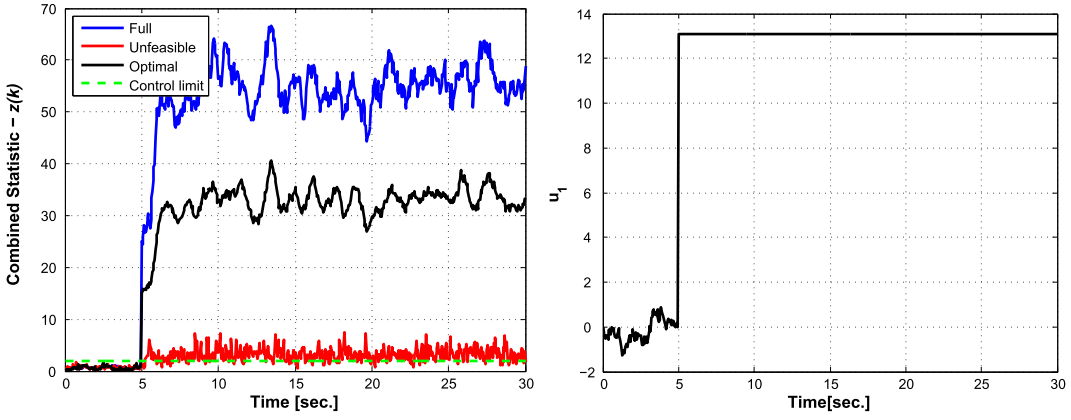

(a) Combined statistic (b) Normalized water to ESR - u_1

Fig. 7 – Fault F_{12} (water to ESR sticking at +5%).

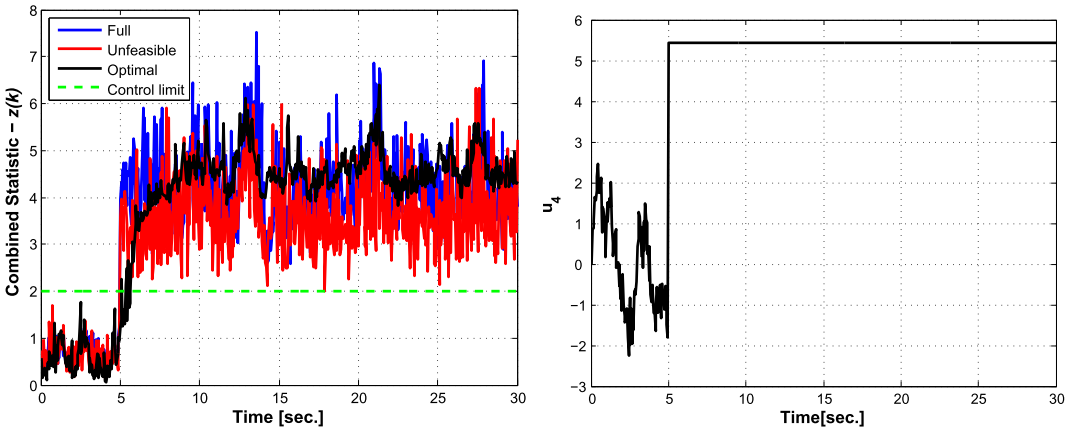

(a) Combined statistic (b) Normalized oxygen to burner - u_4

Fig. 8 – Fault F_{13} (oxygen to burner sticking at +5%).

faults. In this work, the same fault detection is made using only two sensors corresponding to the FC with less time of detection.

Faults F_{12} to F_{15} correspond to failures in manipulated variables, sticking of valves for the first three cases and in the compressor motor voltage for the last one, all at +5%. The combined statistic for these simulations are shown in Figs. 7(a), 8(a) and 9(a) and 10(a) respectively. In all cases the three selections are able to detect the abnormal behavior, although for the twelfth failure, the unfeasible combination has a small percentage of miss detection; again the same selection is slow to detect F_{14}. The more affected manipulated variables for F_{12} and F_{13} are shown in Figs. 7(b) and 8(b), and they correspond to the measurement that is stuck, water to ESR and oxygen to burner respectively. Figs. 7(b) and 8(b) show the water to ESR and stack voltage, which are, correspondingly, the most deviated variables when faults F_{14} and F_{15} occur.

It is important to remark that these faults were studied here in the context of the overall plant which is an important contribution of this work. The same faults considered here for the fuel cell were analyzed previously but this device was isolated. The methodology used here was able to detect the same faults but more quickly and using a less number of measurements. In addition, the same set of measurements chosen initially was able to detect the rest of faults (8) presented here.

Finally, in Table 6 the indicators for the faults analyzed in this work are summarized. Of particular interest is the Fault F_{10} where the optimal monitoring system designed is the only one capable of detecting the abnormal situation, giving a better solution than the full case, which is the most common used in industry. Moreover, this full case implies the maximum hardware investment, because sensors must be bought for every variable that could be measured. And this solution is not even the best from the detectability point of view. So, the solution proposed does not require new sensors (it uses the already installed from the control structure selection stage), and it is able to maximize the fault detection. It

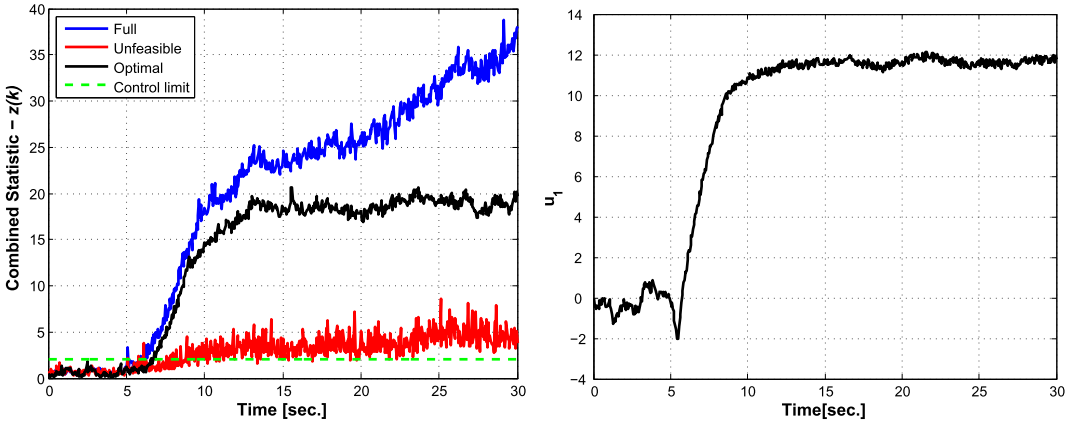

(a) Combined statistic (b) Normalized water to ESR - u_1

Fig. 9 – Fault F_{14} (bio-ethanol to ESR sticking at +5%).

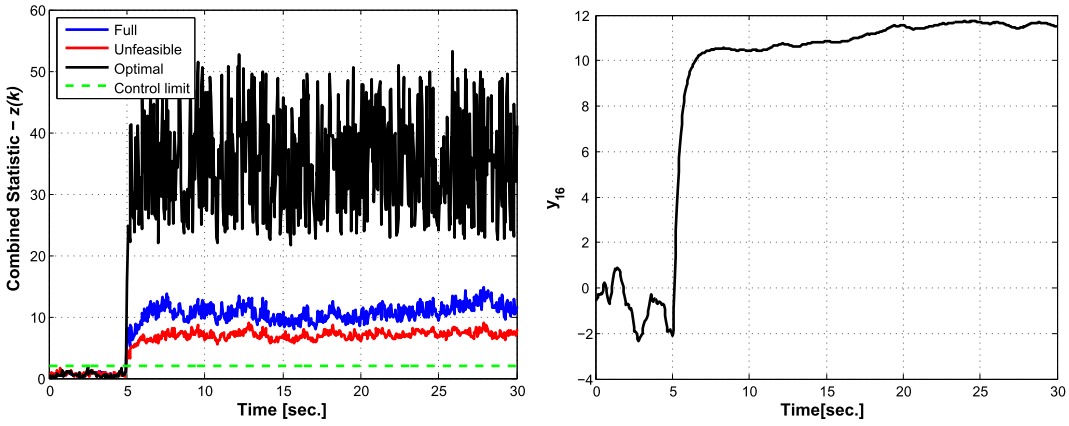

(a) Combined statistic (b) Normalized stack voltage - y_{16}

Fig. 10 – Fault F_{15} (compressor motor voltage sticking at +5%).

does not require extra costs while C_{full} needs the maximum investment, and is not up to the performance of the best solution.

5. Conclusions

A monitoring system for a bio-ethanol processor has been designed using a systematic and generalized approach based on PCA. The optimal number of measurements is selected by using a fault detectability index. This concept is able to reduce the investment cost since the set of measurements can be obtained together with a maximization of the detectability. The results obtained here confirmed that the use of all available measurements for monitoring purposes, is not only superfluous, even more, it can deteriorate the quality of the detectability. The optimal supervisory system is developed using multiple-integrated tools as PCA, combined statistic, detectability analysis, fault subspace extraction and associated investment costs. These elements are included in the objective function so as to promote the use of the existing sensors installed for control purposes. In this work was obtained an optimal solution using only the already existing hardware providing by the control structure. This methodology was firstly applied to detect the most usual faults in seven sensors. In this work the analysis was extended to specific abnormal events inherent to the hydrogen production plant connected to a fuel cell. Hence catalyzer deterioration and troubles in the fuel cell and its auxiliary equipment were tested too. It is demonstrated that the monitoring system is flexible enough to be extended for other faults not considered since the beginning. It was given an integral procedure for an open problem such as the integration of the fault detectability, diagnosis and investment cost analysis in the context of a well driven plant-wide control structure. These advances applied on the hydrogen production system with the FC give the conceptual engineering basis to achieve safety conditions for the overall plant through an integral robust design for this kind of novel and dangerous systems.

Table 6 – Indicators for the last eight faults.

Fault	Design	T_d	RI[%]		Variable
F_8	Full	0.0	91.2	✓	y_6
	Unf	–	16.0	x	
	Opt	0.7	75.0	✓	
F_9	Full	0.0	100.0	✓	u_7
	Unf	0.0	99.0	✓	
	Opt	0.4	98.6	✓	
F_{10}	Full	–	5.6	x	u_7
	Unf	–	18.2	x	
	Opt	0.6	72.2	✓	
F_{11}	Full	1.1	62.2	✓	y_{16}
	Unf	1.0	77.2	✓	
	Opt	0.1	99.6	✓	
F_{12}	Full	0.0	100.0	✓	u_1
	Unf	0.25	82.0	✓	
	Opt	0.0	100.0	✓	
F_{13}	Full	0.0	100.0	✓	u_4
	Unf	0.0	100.0	✓	
	Opt	0.45	98.2	✓	
F_{14}	Full	1.0	96.6	✓	u_1
	Unf	3.7	84.4	✓	
	Opt	1.7	93.4	✓	
F_{15}	Full	0.0	100.0	✓	y_{16}
	Unf	0.0	100.0	✓	
	Opt	0.0	100.0	✓	

Acknowledgments

The authors want to acknowledge the financial support from CONICET (Consejo Nacional de Investigaciones Científicas y Técnicas) and Universidad Tecnologica Nacional-Facultad Regional Rosario from Argentina.

REFERENCES

[1] Casamirra M, Castiglia F, Giardina M, Lombardo C. Safety studies of a hydrogen refuelling station: determination of the

occurrence frequency of the accidental scenarios. Int J Hydrogen Energy 2009;34(14):5846–54.
[2] Kim E, Park J, Cho JH, Moon I. Simulation of hydrogen leak and explosion for the safety design of hydrogen fueling station in korea. Int J Hydrogen Energy 2013;38(3):1737–43.
[3] Kleme JJ, Varbanov PS, Huisingh D. Recent cleaner production advances in process monitoring and optimisation. J Clean Prod 2012;34:1–8.
[4] Aprea JL. Hydrogen energy demonstration plant in patagonia: description and safety issues. Int J Hydrogen Energy 2009;34(10):4684–91.
[5] Yang F, Xiao D. Sensor location strategy in large-scale systems for fault detection applications. J Comput 2008;3(11):51–7.
[6] Bhushan M, Narasimhan S, Rengaswamy R. Robust sensor network design for fault diagnosis. Comput Chem Eng 2008;32(45):1067–84.
[7] Jeong H, Cho S, Kim D, Pyun H, Ha D, Han C, et al. A heuristic method of variable selection based on principal component analysis and factor analysis for monitoring in a 300â kw mcfc power plant. Int J Hydrogen Energy 2012;37(15):11394–400.
[8] Wang D, Romagnoli J. Robust multi-scale principal components analysis with applications to process monitoring. J Process Contr 2005;15(8):869–82.
[9] Hua J, Li J, Ouyang M, Lu L, Xu L. Proton exchange membrane fuel cell system diagnosis based on the multivariate statistical method. Int J Hydrogen Energy 2011;36(16):9896–905.
[10] Nguyen D, Bagajewicz MJ. New sensor network design and retrofit method based on value of information. AIChE J 2011;57(8):2136–48.
[11] Zumoffen D, Basualdo M. A systematic approach for the design of optimal monitoring systems for large scale processes. Ind Eng Chem Res 2010;49(4):1749–61.
[12] Nieto Degliuomini L, Zumoffen D, Basualdo M. Plant-wide control design for fuel processor system with PEMFC. Int J Hydrogen Energy 2012;37(19):14801–11.
[13] Yue HH, Qin SJ. Reconstruction-based fault identification using a combined index. Ind Eng Chem Res 2001;40:4403–14.
[14] Li W, Yue H, Valle-Cervantes S, Qin S. Recursive PCA for adaptive process monitoring. J Process Contr 2000;10:471–86.
[15] Zumoffen D, Basualdo M. From large chemical plant data to fault diagnosis integrated to decentralized fault-tolerant control: pulp mill process application. Ind Eng Chem Res 2008;47(4):1201–20.
[16] Zumoffen D, Basualdo M. Improvements in fault tolerance characteristics for large chemical plants. Part I: waste water treatment plant with decentralized control. Ind Eng Chem Res 2008;47(15):5464–81.
[17] Zumoffen D, Basualdo M, Molina G. Improvements in fault tolerance characteristics for large chemical plants. Part II: pulp mill process with model predictive control. Ind Eng Chem Res 2008;47(15):5482–500.
[18] Wold S. Exponentially weighted moving principal components analysis and projection to latent structures. Chemometr Intell Lab 1994;23:149–61.
[19] Ruiz D. Fault diagnosis in chemical plants integrated to the information system. Ph.D. thesis. España: Departament d'Enginyeria Química, Escola Técnica Superior d'Enginyers Industrials de Barcelona, Universitat Politécnica de Catalunya; March 2001.
[20] Musulin L, Puigjaner E. Abnormal situation management. Germany: LAP LAMBERT Academic Publishing GmbH& Co. KG; 2012.
[21] Chiang L, Pell R, Seasholtz M. Exploring process data with the use of robust outlier detection algorithms. J Process Contr 2003;13:437–49.
[22] Basualdo M, Feroldi D, Outbib R. PEM fuel cells with bio-ethanol processor systems. Springer; 2012.
[23] Zumoffen D, Basualdo M. Fault detection systems integrated to fault-tolerant control. Application to large-scale chemical processes. Germany: LAP LAMBERT Academic Publishing GmbH& Co. KG; 2012.